Int J Appl Earth Obs Geoinformation 67 (2018) 98–113

Contents lists available at ScienceDirect

Int J Appl Earth Obs Geoinformation

journal homepage: www.elsevier.com/locate/jag

Seagrass mapping in Greek territorial waters using Landsat-8 satellite images

Konstantinos Topouzelis*, Despina Makri, Nikolaos Stoupas, Apostolos Papakonstantinou, Stelios Katsanevakis

Department of Marine Science, University of the Aegean, University Hill, 81100, Mytilene, Greece

ARTICLE INFO

Keywords:
Posidonia oceanica
Object based image analysis (OBIA)
Landsat-8
Marine habitat

ABSTRACT

Seagrass meadows are among the most valuable coastal ecosystems on earth due to their structural and functional roles in the coastal environment. This study demonstrates remote sensing's capacity to produce seagrass distribution maps on a regional scale. The seagrass coverage maps provided here describe and quantify for the first time the extent and the spatial distribution of seagrass meadows in Greek waters. This information is needed for identifying priority conservation sites and to help coastal ecosystem managers and stakeholders to develop conservation strategies and design a resilient network of protected marine areas. The results were based on an object-based image analysis of 50 Landsat-8 satellite images. The time window of image acquisition was between June 2013 and July 2015. In total, the seagrass coverage in Greek waters was estimated at 2619 km^2. The largest coverages of individual seagrass meadows were found around Lemnos Island (124 km^2), Corfu Island (46 km^2), and East Peloponnese (47 km^2). The accuracy assessment of the detected areas was based on 62 Natura 2000 sites, for which habitat maps were available. The mean total accuracy for all 62 sites was estimated at 76.3%.

1. Introduction

Seagrass meadows are among the most valuable coastal ecosystems due to their structural and functional roles in the coastal environment. In recent years, seagrass meadows have become among the main targets of conservation efforts in European waters. *Posidonia oceanica* is an important endemic species in the Mediterranean Sea, which can form meadows extending from 0 to 40–45 m depth (Telesca et al., 2015). *P. oceanica* is one of the priority habitats of the European Union's (EU's) Habitats Directive (92/43/EEC) and it is protected by the Barcelona Convention. Furthermore, the EU Mediterranean Fisheries Regulation (EC No. 1967/2006) requires mapping highly important habitats for fish production, (such as seagrass meadows), in all EU member states, and imposes restrictions to fishing activities in such habitats.

The *World Atlas of Seagrasses* (Green and Short, 2003), a publication developed in collaboration with the United Nations Environmental Program-World Conservation Monitoring Center (UNEP-WCMC), tried to synthesize seagrass distribution on a global scale. Greece is almost absent in that report due to lack of information.

The most recent study on seagrass meadows in the Mediterranean Sea (Telesca et al., 2015) presented the historical distribution of *P. oceanica* and the total area of seagrass meadows. According to Telesca et al. (2015), only 8% of the Greek coastline was surveyed, and the known *P. oceanica* cover in Greek territorial waters totaled 44,939 ha (449.39 km^2). Taking into account the total coastal length of Mediterranean Sea without sea grass data (21,471 km) and the unmapped coastal length of the Greek coastline (≈14,000 km), almost 65% of the unmapped potential seagrass areas of Mediterranean Sea are in Greek waters. Previous studies on seagrass mapping in the Mediterranean Sea had either a limited spatial extent (Boudouresque et al., 2009) or provided maps at a low spatial resolution (Giakoumi et al., 2013).

The only areas in Greek territorial waters for which detailed habitat maps are available are 62 marine sites of the Natura 2000 network. These sites, with a large coverage of seagrass meadows, were extensively mapped between 1998 and 2001. For each area, a dedicated map was produced using a combination of *in situ* measurements, including phytobenthic sample analysis, hydroacoustic sensors for seabed classification (RoxAnn), underwater photography/video and aerial imagery (Panayiotidis et al., 2002). Although the Hellenic Centre for Marine Research (HCMR) systematically monitors the health status of seagrass meadows in Greece, their geographic distribution has rarely been mapped. The statistics on the lower limits and the meadow densities of *P. oceanica* in the Greek seas were reported (Gerakaris et al., 2014), however, the produced datasets are not available in the geographic information systems (GIS) format. Finally, the marine part of Samaria National Park on Crete Island was mapped using mainly

* Corresponding author.
E-mail address: topouzelis@marine.aegean.gr (K. Topouzelis).

https://doi.org/10.1016/j.jag.2017.12.013
Received 16 October 2017; Received in revised form 20 December 2017; Accepted 25 December 2017
0303-2434/

echosounder data (Poursanidis et al., 2014).

Remote sensing permits the study of extensive coastal areas for assessment of the spatial patterns of seagrass meadows, and simultaneously can be used to reveal temporal patterns due to the high frequency of the observation (Green et al., 2000). Mapping seagrass meadows from space on a large scale cannot provide the levels of accuracy and detail of a field survey. However, the complete area coverage of satellite images provides benefits by revealing large-scale patterns (Hedley et al., 2016). Remote sensing covers a variety of technologies from satellite images, aerial systems, boat systems, and underwater remotely operated vehicles (ROVs). The power of remote sensing techniques has been highlighted by the estimation of the statistical power of mapping coastal areas. Mumby et al. (2004) implied that 20 s of airborne acquisition time would equal 6 days of a field survey. Hossain et al. (2015) presented an overview of the extent of the remote sensing of seagrass ecosystems. Four parameters were mapped from remote sensing data: presence/absence, percentage coverage, species, and biomass. The selection of the most relevant parameter in the scientific literature depended on the area mapped, the availability of ground truth data, and the specific target of each study (e.g., ecology, change detection).

Although seagrass mapping with high-resolution satellite images is common in relatively small areas, only a few studies (Monaco et al., 2012; Torres-Pulliza et al., 2013; Wabnitz et al., 2008) have focused on a regional-scale mapping with low-resolution data. The feasibility of achieving large-scale seagrass mapping from Landsat images with acceptable accuracies was first presented by Wabnitz et al. (2008) for the Wider Caribbean region. Later, the Lesser Sunda Ecoregion (LSE) in the Coral Triangle (tropical marine waters of Indonesia, Papua New Guinea, Philippines, Solomon Islands and Timor-Leste) was mapped to support the design and implementation of protected marine areas using 18 Landsat scenes (Torres-Pulliza et al., 2013). A recent publication by the National Oceanic and Atmospheric Administration (NOAA) reported on the long-term mapping of the shallow-water coral reef ecosystems across the US (Monaco et al., 2012). Although this report was dedicated to US territory, it detailed the methodologies used, the results of habitat mapping (including the exceptional study on Puerto Rico and the US Virgin Islands), and the national statistics.

The 30-m resolution of Landsat images was previously used successfully for regional mapping. This paper reports for the first time on the seagrass beds' distribution in Greek waters by using a consistent method. Despite the increasing number of studies on seagrass mapping with satellite data, relevant data in GIS formats are still difficult to access. This study explains the production of country-scale seagrass GIS vectors, derived from Landsat-8 imagery. The results are compared with the data from national reference maps, provided for protected areas. Finally, the products' relevance for future biodiversity research on conservation and management at the country level is discussed.

2. Materials and methods

2.1. Area of study

The area of study (Fig. 1) spans the national marine territorial borders of Greece, covering 13,676 km of coastline, in the Aegean Sea, the eastern Ionian Sea, and the northern Libyan Sea. The study area can be divided into three major regions regarding the deep-limit of seagrass (Gerakaris, 2017; Gerakaris et al., 2014): the Northern Aegean Sea, the Southern Aegean Sea, and the Ionian Sea with depth limits 26.3 m (± 6.44 m), 30 m (± 5.75 m), and 35.4 m (± 4.95 m) respectively. The northern Aegean Sea consists of shallow platforms, resulting from the offshore continuation of the alluvial plains of northern Greece. These plains are fed with terrigenous clastic material because of river drainage (Sakellariou et al., 2005). The North Aegean Sea is also a dilution basin, as the water balance is positive; fresh light waters come from the Black Sea through the Dardanelles Strait. The South Aegean Sea is a concentration basin, as the water balance is negative, and evaporation exceeds freshwater input. The Aegean Sea is characterized by a complex geomorphological status as a result of geological and geodynamic processes (Sakellariou and Alexandri, 2007). The Aegean Archipelago comprises a group of islands, including Cyclades southeast of mainland Greece, Sporades along the east coast, Dodecanese on the eastern limit of the Cretan Sea, and the northeastern Aegean Islands (the major ones are Ikaria, Samos, Chios, Lesvos, Limnos, and Samothrace). The Ionian Sea is located on the western part of Greece, south of the Adriatic Sea, and covers the Ionian Islands (the main ones are Corfu, Zakynthos, Kefalonia, Ithaca, and Lefkada) and the west coast of Peloponnese. On the southern part of the study area, the sea floor morphology and sedimentation are controlled by the seismicity of the region. Normal active faults can cause the formation of deep bays, such as the Messiniakos and the Lakonikos Gulfs (Sakellariou et al., 2005). Finally, the Cretan Sea is located between Santorini Island and Crete Island. The sea area around Crete can also be divided into the northern part toward the Aegean Archipelago and the southern part toward the Libyan coast (*i.e.*, the Libyan Sea). In Crete, a deep basin called Heraklion Basin can be found, with a depth of about 1800 m.

2.2. Image dataset

The present study is based on Landsat-8 satellite images (Operational Land Imager; OLI). Landsat-8 was launched in February 2013 and has a repeat cycle of 16 days, with an approximate scene size of 170 km (north-south) to 183 km (east-west). The OLI sensor operates on seven bands, from coastal blue (0.43–0.45 μm) to SWIR2 (2.11–2.29 μm), with a 30-m spatial resolution and a 12-bit radiometric resolution. The data are available free of charge via an HTTP download within 24 h of acquisition. As opposed to previous Landsat sensors, the Landsat-8 series included the coastal blue band, which is dedicated to images of shallow waters (https://lta.cr.usgs.gov/L8).

Landsat-8 collects images with a standard world reference system (WRS-2). Greece is covered in 33 frames (row/path), of which 25 cover all the Greek coastal or marine areas (Fig. 2). During the time window from June 2013 to July 2015, in total, 50 Landsat-8 images were downloaded for further processing (Table 1). The images were chosen manually based on three basic quality criteria: i) cloud-free images, ii) calm seas as possible (or low and stable wind speed), and iii) the absence of major oceanographic phenomena (e.g., fronts, eddies). However, due to the large swath of Landsat-8 images and the complexity of the Aegean Sea, in many cases, the criteria were not fulfilled. Some of the images were ideal for further processing, while others depicted oceanic phenomena that prevented accurate seagrass mapping. Therefore, each Landsat-8 frame (path and row) was covered by two images. At the classification stage, the first image was processed for seagrass mapping; for all subareas where the water clarity was insufficient, the second image was taken instead. During the image-selection phase, a strong preference was given for the period between months of August and December or close to them due to better water stratification (*i.e.* thermocline reaches maximum). The images were explored and downloaded from the United States Geological Survey (USGS) Earth Explorer web service (http://earthexplorer.usgs.gov).

2.3. Image analysis

The methodological framework was based on four main pillars (Fig. 3), as follows: (i) the data selection contained Landsat-8's frame identification as described in the previous paragraph; (ii) the pre-processing phase included all the necessary steps for the main analysis (*i.e.*, radiometric calibration, atmospheric correction, land mask, and image cropping); (iii) the object-based image processing, the images segmented into objects, classified, and manually edited where necessary; (iv) finally, in the accuracy assessment, the quality of the product was assessed.

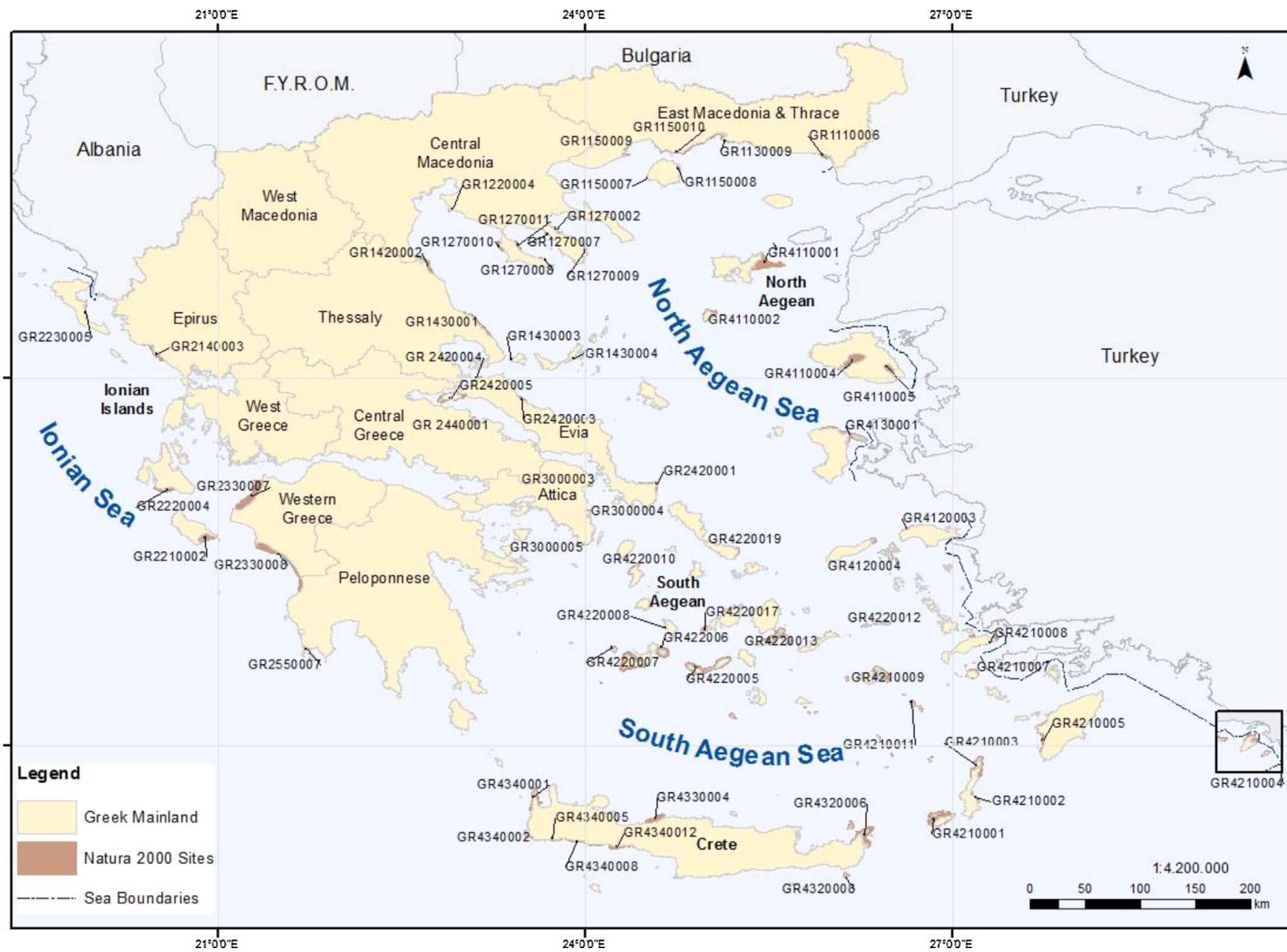

Fig. 1. Map of the study areas with the Greek territorial waters and the sites of accuracy assessment containing P. oceanica meadows derived from Natura 2000 network with their seven-digit codes.

2.3.1. Preprocessing phase

The preprocessing phase was necessary for producing images with as similar characteristics as possible for the main processing phase. It was designed as a chain of four processes: i) radiometric calibration, ii) atmospheric correction, iii) land masking, and iv) image cropping according to the Greek mapping system on a scale of 1:50,000.

Radiometric calibration was required for transporting the images' digital numbers (DNs) to the top of atmosphere (TOA) radiance values (in $\mu W/cm^2*nm*sr$) and preparing the image format for the next stage of atmospheric correction (USGS, 2016). The atmosphere's influence on the satellite images was corrected by using the Fast Line-of-sight Atmospheric Analysis of Spectral Hypercubes (FLAASH©) toolbox of the ENVI© 5.2 software (Matthew et al., 2002). The three main parameters of the FLAASH© atmospheric model, aerosol model, and aerosol retrieval were mid-latitude summer (or tropical in the summer months), maritime model, and two-band over water, respectively. The resulting reflectance images (independent of season, zenith and azimuth angles) were used for further processing.

Land masking was performed by using the Water Index (WI), calculated as the fraction of the difference between coastal plus near infrared band to coastal plus infrared band (Wolf, 2010). The used threshold was WI > 0, which is the typical threshold for standing water in a pixel. This band combination was first designed for WorldView-2 images to highlight areas of standing water greater than one pixel in size; however, it was quite satisfactorily applied to the Landsat-8 images.

The final stage of the preprocessing phase was the selection of the coastal areas. Seagrass meadows do not extend beyond 40 m in depth (Gerakaris et al., 2014). Therefore, only coastal areas had to be analyzed. The Landsat-8 images were also cropped, using the map borders of the Hellenic Military Geographical Service (HMGS) on a scale of 1:50,000 (Fig. 2). A three-digit code (*i.e.*, FXCODE) was used for reference selection. The last step was twofold. First, the large images were cropped into smaller areas, making them easier to handle in the complicated environment of the study area. Second, the images (e.g., specific FXCODES) without good water conditions were replaced by the second set of available images.

2.3.2. Object-based image analysis

Once preprocessed, the Landsat-8 images were imported to the main processing phase, where the detection of seagrass ensued. The detection was a result of a supervised fuzzy classification technique and where necessary, of manual editing. We employed the object-based image analysis (OBIA), where the images were first segmented into objects with the same spectral characteristics and then classified according to predefined rules. We used the eCognition Developer v 9.2 software; the produced ruleset is available on request. The approach from Lyons et al. (2012) was adapted to the environmental conditions and data used in this study *i.e.* multiple level of segmentations, hierarchical classes, rules with fuzzy memberships and thresholds.

From the nine bands of Landsat-8 OLI, only the first four (*i.e.*, coastal, blue, green, and red) were used for the seagrass detection. This selection was a result of the wavelengths' inherent capabilities to penetrate the clean sea water. Red band was used to discriminate seagrass from reefs in shallow waters. Fig. 4 presents the flow chart of the designed methodology, organized into three steps: i) coastal area

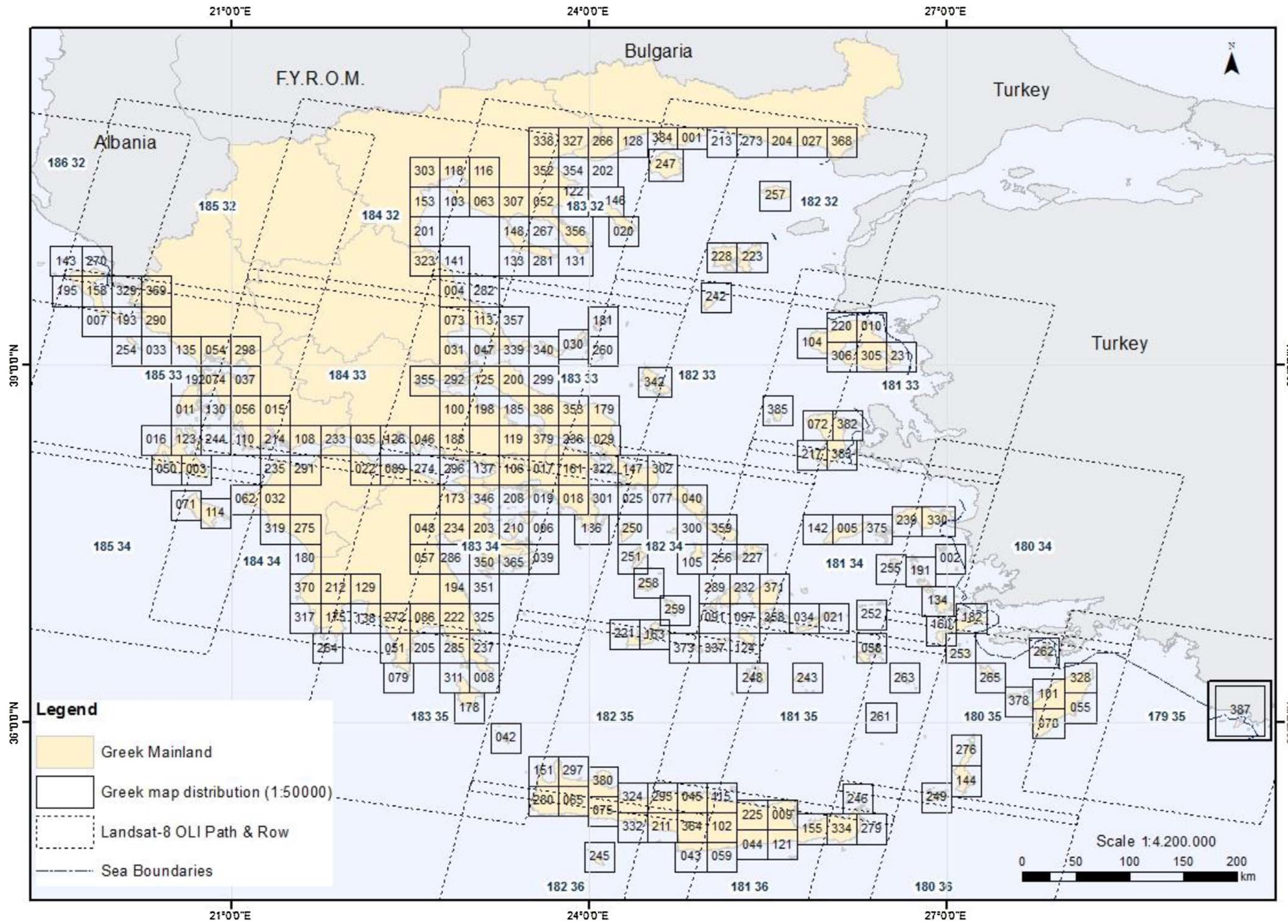

Fig. 2. Landsat-8 reference system over Greece with the frames (row/path). With dashed line the study areas as covered by the 25 Landsat-8 frames showing the Hellenic waters. Distribution of selected coastal areas based on the Hellenic Military Geographical Service map sheets on a scale of 1:50,000, with the three-digit reference code.

Table 1
Dataset of Landsat-8 images selected for analysis.

No	Path	Row	Date-1	Date-2
1	179	35	27/08/2014	13/07/2015
2	180	34	24/12/2014	07/04/2015
3	180	35	01/07/2014	24/12/2014
4	180	36	24/12/2014	07/01/2014
5	181	32	10/09/2014	24/05/2015
6	181	33	21/05/2014	09/10/2014
7	181	34	08/07/2014	25/06/2015
8	181	35	25/08/2014	25/06/2015
9	181	36	03/04/2014	25/06/2015
10	182	32	29/06/2014	19/10/2014
11	182	33	15/05/2015	29/08/2013
12	182	34	01/09/2014	31/05/2015
13	182	35	31/07/2014	16/06/2015
14	182	36	31/07/2014	16/08/2014
15	183	32	09/07/2015	23/08/2014
16	183	33	01/04/2014	20/08/2013
17	183	34	14/01/2015	22/07/2014
18	183	35	22/07/2014	07/06/2014
19	184	32	01/10/2014	14/08/2014
20	184	33	15/08/2014	24/06/2013
21	184	34	14/08/2014	11/04/2015
22	185	32	04/05/2015	07/04/2014
23	185	33	20/07/2014	07/04/2014
24	185	34	05/08/2014	05/04/2014
25	186	32	28/08/2014	08/12/2014

selection, ii) broad classification, and iii) detailed classification. The coastal area selection was based on the operator selection of large predefined areas. These areas resulted from a large chessboard segmentation (scale of 200), representing coastal areas with the possibility of having seagrass. Once the areas were selected manually, they were merged into one large segment. This segment would be the specific area of FXCODE to which the rest of the steps would apply. With this design, a large part of each FXCODE containing deep waters would be excluded from further analysis.

The second step of broad classification divided the area of interest into three basic classes: “shallow areas”, “deep sea”, and “possible seagrass”. For this step, a multiresolution segmentation was applied with the broad scale of 50, and the produced objects were grouped into the three classes by using thresholds. For the class “shallow areas”, the blue (B) and the green (G) channels were used ($0.6 < B/G \leq 1$), while for the class “deep sea”, the red (R) channel was also necessary ($B/G \geq 1.5$, $G/R \leq 1.3$, and $500 \leq (B*R)/G \leq 600$). Red channel has relative stable water reflectance in deep waters and it was used as complementary band for calculating the spectral indexes. The remaining objects were classified as “possible seagrass”. The segments that were classified under the same category were then merged, and the two categories (possible seagrass and coastal area) were further processed in the last step.

In the third step, a detailed classification was necessary for detecting the small seagrass patches on coastal areas and for identifying small discontinuities (e.g., sandy areas or rocky substrates) among seagrass meadows (*i.e.*, to describe the coastal area better). A new multiresolution segmentation was applied with the scale of 30, and a

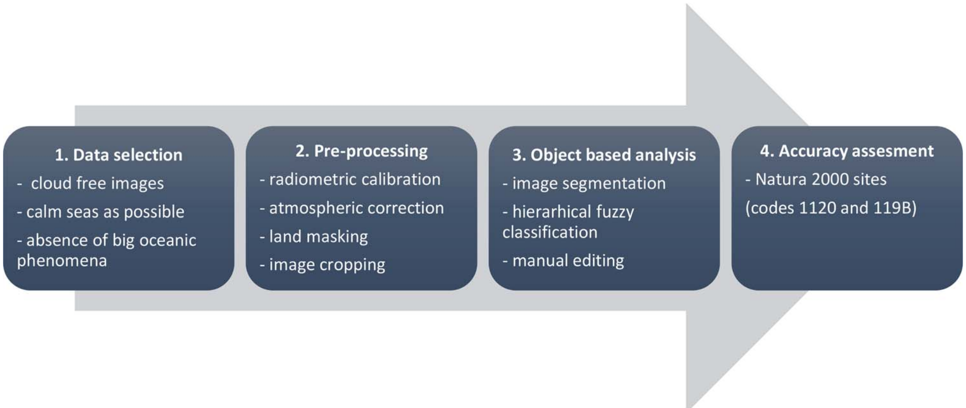

Fig. 3. Methodological framework for data analysis.

small meaningful object was created for shallow areas (without seagrass) and possible seagrass categories. In this step, several subcategories were created, and fuzzy logic rules were used for every subcategory. The limits of the rules derived from the samples of each subcategory were manually defined during the training phase. The rules were based on the four available bands and differed for each class category. For example, the seagrass class and their subcategories used the mean values of bands Coastal, Blue and Green (C, B and G respectively) and their combinations (e.g., C*B, B*G/R). In total, seagrass and coastal areas contained seven and five fuzzy rules, respectively (Fig. 5). The designed classification methodology produced satisfactory results in coastal areas when the coastline was relatively simple. In more complex cases or with high turbid waters, manual classification was necessary for producing results with high accuracy. For each FXCODE, a dedicated vector was created with a specific code name: FXCODE_row_path_date (e.g., 148_183_32_20140823). Where necessary, the second image of the same area was examined (*i.e.*, the same FXCODE but a different date), and the results of both images were compared for

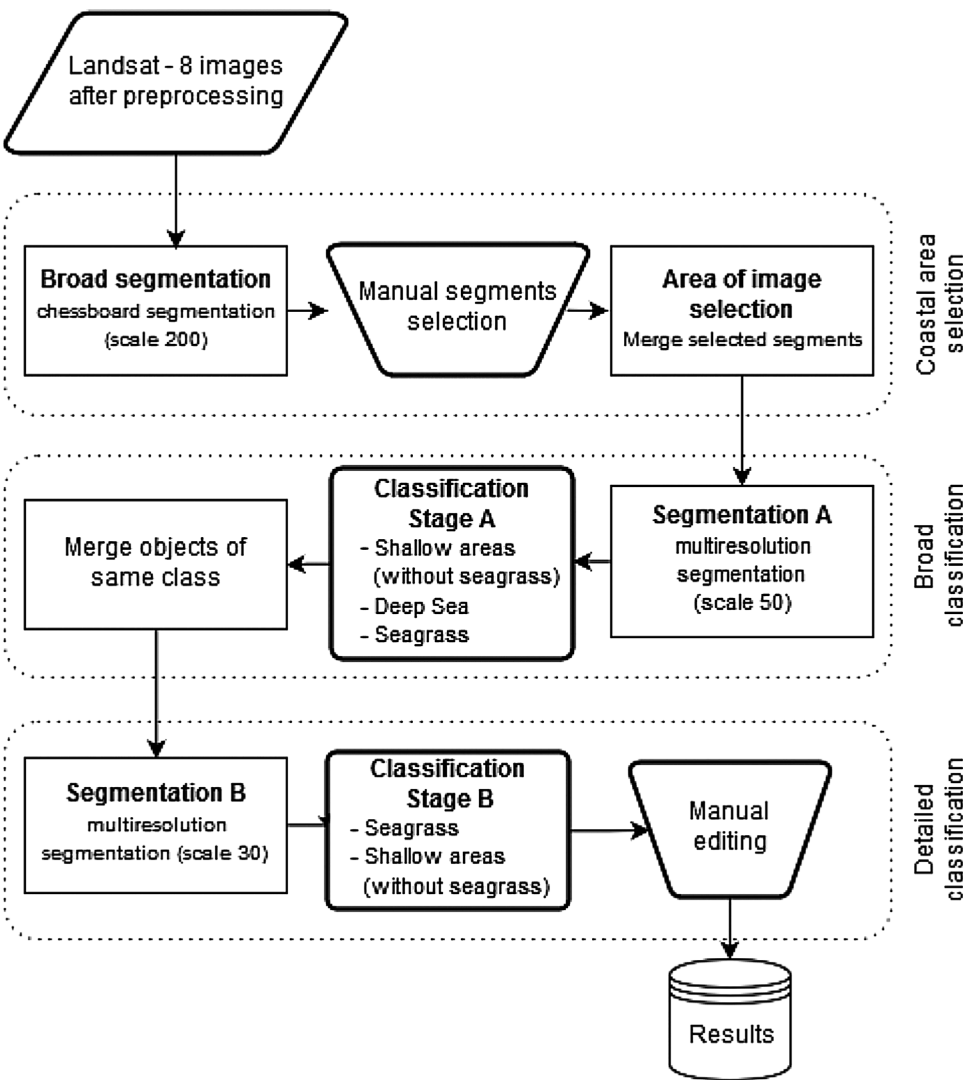

Fig. 4. Flow chart of the designed methodology based on object-based image analysis.

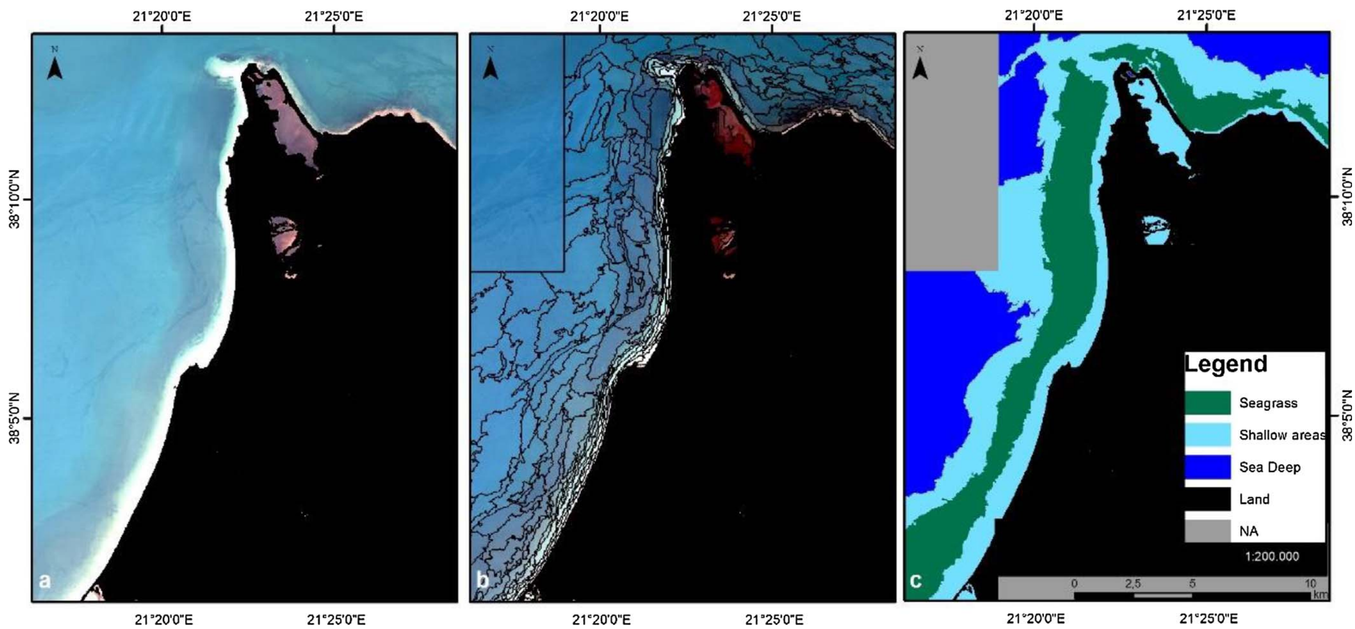

Fig. 5. An example of the results. a) Image after preprocessing step, b) object-based image analysis, c) classification of the object into subtidal seagrass (green), coastal shallow areas (light blue), and deep sea (blue). (For interpretation of the references to colour in this figure legend, the reader is referred to the web version of this article.)

their significance. The user does not need to have prior knowledge about the desired objects *i.e.* seagrass or substrate/bottom types.

2.3.3. Accuracy assessment scheme

An accuracy assessment requires *in situ* measurements in the area of study. Traditionally, these measurements can be underwater photographs or videos taken during snorkeling or scuba diving, sound equipment (side scan sonar, multibeam), drop cameras, underwater ROVs, or even high-resolution satellite images in relatively shallow waters.

The accuracy assessment was based on the Greek national maps produced under the Natura 2000 framework. Natura 2000 is an EU network consisting of special areas of conservation (SACs) and special protection areas (SPAs), designed for each EU country under the Habitats Directive and the Birds Directive, respectively. The Natura 2000 network includes both terrestrial and marine sites. Greece has 62 coastal areas in the Natura 2000 network, most of them with a large coverage of seagrass meadows. Similar to all the Natura 2000 network sites, these areas were named with the country prefix and a seven-digit code, for example, GR2420005 (Fig. 1). The coastal Greek Natura 2000 sites are distributed in all Greek territorial waters, from the northern turbid waters of the Macedonia coast to the southern clean waters on Crete Island.

Each produced map contains several classification categories, of which two were used for the accuracy assessment: the *P. oceanica* beds (code category 1120) and the soft substrates with vegetation (code category 119B). The first one clearly indicates the meadows of *P. oceanica*, since these are among the protected species. The second one refers to areas containing other angiosperms, such as *Cymodocea nodosa*, *Zostera noltii,* and *Zostera marina*.

For each of the 62 Natura sites (Fig. 1), the produced vector with the seagrass was compared with the one from the Natura 2000 mapping, and a confusion matrix was created (Congalton and Green, 2008). Since the accuracy estimation referred to the two-class problem (seagrass and non-seagrass), the total accuracy for each site was calculated as the sum of the areas of correctly classified 'seagrass' and correctly classified 'non-seagrass' divided by the total area of 'seagrass' and 'non-seagrass' in the Natura 2000 reference mapping. However, because overall accuracy was sometimes biased by the size of the non-seagrass class the common area of seagrass between the produced vector and the Natura 2000 vectors was calculated (area in km^2 and % coverage) and is presented in Table 2.

The produced vectors were examined for identifying the deepest limit of seagrass meadows in each sub-area of the study. For estimating the deep limit of the seagrass meadows, the Hellenic Navy Hydrographic Service's (HNHS) isobaths with 10 m interval (*i.e.* 10-m, 20-m, 30-m, 40-m) were used as reference.

3. Results

The result of the analysis was a group of vectors (presence or absence) of seagrass for each subarea of interest (*i.e.* ESRI shapefile). Individual neighboring vectors were merged to calculate the statistics for the Greek waters. The produced vector layer can be downloaded from the University of Aegean's Marine Remote Sensing Group web page http://mrsg.aegean.gr/ and from ZENODO database (DOI:10.5281/zenodo.1120338). Each vector contains information on the processed area in which it belongs (FXCODE), and information on the processed Landsat-8 image (path/row and acquisition date).

3.1. General observations

In total, the seagrass coverage over Greek waters was estimated at 2,619.25 km^2, of which 1,432.54 km^2 were detected in the north part and 1,186.72 km^2 in the south part of the territorial waters.

Fig. 6 presents the distribution of the seagrass coverage over the study area. The total areas of seagrass coverage were about 330.6 km^2 in the Peloponnese, 315 km^2 in the group of Cyclades Islands, 206 km^2 in Dodecanese, and 145 km^2 in Crete. There were extensive areas of seagrass beds along the Greek shoreline, some of which could be found at depths up to ~40 m. The largest coverage of individual seagrass meadows was found around Lemnos Island (124 km^2), although the island is not one of the largest in Greece. Next on the list of the larger individual meadows were the northern part of Corfu (46 km^2), East Peloponnese (47 km^2), Thasos Island (46 km^2), and Kos Island (38 km^2). Adding separate but neighboring seagrass meadows revealed new meaningful areas (e.g., Corfu Island and Peloponnese). Corfu Island (116 km^2) had two large seagrass areas, the first on the northwest part of the island (55.6 km^2) and the second on the south part (50 km^2). Adding the separate parts of Peloponnese revealed a large coverage of

Table 2
Accuracies and errors of the produced seagrass coverage for the Greek reference coastal Natura 2000 sites.

Natura 2000 Sitecode	Natura 2000 sea area (km^2)	Natura 2000 seagrass area (km^2)	Seagrass detected (km^2)	Seagrass detected (%)	Total accuracy (%)
GR1130009	105.57	0.68	0.60	87.46	92.67
GR1150007	2.08	0.40	0.33	82.17	53.99
GR1150008	4.49	1.78	1.43	80.41	74.69
GR1150009	16.22	2.28	1.37	60.30	81.54
GR1220004	3.81	1.27	0.65	51.11	75.86
GR1270002	11.65	6.36	2.26	35.59	56.56
GR1270007	5.44	3.83	1.78	46.54	54.40
GR1270008	3.00	1.06	0.51	48.13	78.05
GR1270009	11.34	9.13	1.24	13.63	29.54
GR1270010	20.25	7.39	2.31	31.20	67.51
GR1270011	10.12	2.90	1.03	35.44	79.94
GR1420002	28.54	2.06	1.50	72.59	85.99
GR1430001	30.11	1.19	0.46	38.81	93.22
GR1430003	0.58	0.33	0.16	48.32	57.28
GR1430004	22.48	17.07	3.72	21.76	38.80
GR2140003	40.09	5.79	1.23	21.24	84.98
GR2210002	61.93	26.29	16.93	64.40	79.43
GR2220004	40.52	14.72	7.33	49.79	73.12
GR2230005	8.92	7.32	2.58	35.33	44.80
GR2330007	158.69	51.54	42.40	82.27	77.21
GR2330008	163.31	28.66	2.33	8.13	74.58
GR2420001	15.56	6.74	0.85	12.61	60.60
GR2420003	8.23	2.41	0.15	6.23	64.16
GR2420004	8.00	0.55	0.47	85.33	95.17
GR2420005	53.48	25.18	1.94	7.70	55.54
GR2440001	13.80	3.48	0.29	8.44	64.78
GR2550007	11.91	4.68	2.09	44.70	70.36
GR3000003	13.21	2.36	0.84	35.53	93.87
GR3000004	4.85	1.95	1.18	60.38	73.20
GR3000005	19.22	6.13	4.79	78.09	60.56
GR4110001	130.09	115.07	95.39	82.90	80.92
GR4110002	24.15	5.43	2.28	41.87	67.69
GR4110004	118.73	2.88	1.63	56.82	93.64
GR4110005	45.58	4.90	0.37	7.53	89.47
GR4120003	4.46	1.09	0.43	39.59	78.03
GR4120004	52.55	5.43	2.41	44.39	90.83
GR4130001	64.29	21.60	6.96	32.20	64.00
GR4210001	122.49	19.40	16.05	82.71	74.80
GR4210002	13.45	0.81	0.44	54.08	79.63
GR4210003	58.93	2.79	1.43	51.21	92.69
GR4210004	18.48	2.14	0.23	10.77	89.50
GR4210005	47.83	10.68	5.57	52.13	72.28
GR4210007	17.33	3.20	1.47	45.92	77.78
GR4210008	22.91	7.90	2.71	34.32	57.09
GR4210009	60.93	0.90	0.13	14.49	97.96
GR4210011	54.04	0.07	0.01	14.64	99.15
GR4220005	230.95	7.33	4.72	64.35	90.09
GR4220006	52.53	0.31	0.12	38.64	85.11
GR4220007	9.17	0.03	0.01	39.22	89.53
GR4220008	2.55	1.16	0.28	24.06	61.96
GR4220010	13.26	3.93	0.46	11.70	73.53
GR4220012	41.73	3.79	0.03	0.79	90.80
GR4220013	137.90	37.45	10.46	27.93	79.67
GR4220017	17.13	5.96	2.93	49.16	77.29
GR4220019	7.90	2.17	0.44	20.31	75.19
GR4320006	119.39	6.28	0.98	15.59	92.70
GR4320008	8.84	0.05	0.00	6.00	87.33
GR4330004	57.04	10.04	1.48	14.74	72.60
GR4340001	51.75	1.94	0.60	30.93	95.85
GR4340005	10.80	0.07	0.03	43.40	97.50
GR4340008	37.13	0.17	0.02	11.97	94.40
GR4340012	35.59	0.83	0.60	72.11	68.28

86 km^2.

In terms of seagrass coverage (km^2) of the Greek administrative regions, Southern Aegean had by far the largest coverage with almost 600 km^2, followed by the Ionian Islands with 440 km^2. Only two other regions had coverage larger than 200 km^2 (*i.e.*, Northern Aegean and Western Greece with 301 km^2 and 254 km^2, respectively).

The designed methodological process was robust and worked satisfactorily in most of the cases. The sub-division of the study area using the Greek mapping system on the 1:50,000 scale was found very effective because of small variations on the sea state (e.g. clarity, turbidity, waves) in each sub-area. In the case of unclear substrate the second Landsat-8 image was used. Consequently, the classification was more effective and accurate in each sub-area. However, due to the very large study area, the differences in the sea state were very common from sub-area to sub-area, and in most of the cases manual processing was necessary to add or remove small image segments. The automatic procedure was effective in detecting the large meadows but was unsuccessful in small patches because of the signature difference due to depth variation. Depth invariant indexes could have worked in this direction. The northern part of the study area (regions of Central Macedonia, Eastern Macedonia and Thrace, and Northern Aegean) presented higher difficulties regarding detection than the rest of the study area (i.e. South Aegean and Ionian Sea). This is most probably due to water clarity and comes in line with the difference of the seagrass depth limit from the northern to southern part of the study area. Another important issue was the nature of the Greek shoreline, which follows a complex shape with small bays and large depth differences. This particularity affected the results of the classification process in relatively small meadows especially when both images (the same subarea looked by two different days) were processed. Although the 30 m spatial resolution can reveal a good overview of the presence of the seagrass meadows, a better spatial resolution is required to monitor the trends in seagrass coverage.

One of the interesting findings of this work was the estimation of the deep limit of seagrass meadows in the Hellenic waters. As mentioned above the Hellenic Navy Hydrographic Service's (HNHS) 10-m isobath was used as the reference for the depth. The deepest points were located as follows: in Peloponnese on the southeastern and the northwestern edges (close to 30 m in depth), in Dodecanese on Kos Island (20 m), in Cyclades on Santorini Island (over 30 m), and on the northern part of Crete Island (close to 40 m). Detection vectors were produced with a defined geometry which many times followed the isobath of HNHS. The limit of the meadows was clearly defined in most cases, even with a small color difference between deep limit and deep water. In the north and northeast parts of Greece (in the regions of Central Macedonia, Eastern Macedonia and Thrace) the detected deep limit of the seagrass meadows was underestimated due to turbid waters.

For estimating the validity of the depth detection, one of the deepest detected meadows in South Crete was further investigated (Fig. 7). For this case study, a more accurate depth contour was used (derived by single beam echosounder and extrapolated in 5-m isobath). As can be seen, the larger meadow located in the northern part of the image ends close to 40 m depth in two points, and the southern smaller meadow goes even deeper. Taken into account the uncertainties due to positioning errors and the image spatial resolution, 40 m was considered a valid depth limit. The seagrass meadow is visible in such depth even with a small color difference. The automatic procedure was unsuccessful to detect it, exactly because of the small spectral difference in the neighbouring area, and manual classification was performed. The preconditions for the detection in such deep waters are very clean waters, calm sea surface conditions, a combination of Coastal, Blue and Green bands for the classification, and the high radiometric resolution of Landsat-8 images. The first two are environmental parameters which should be met during the image acquisition, the fourth is determined from the Landsat's-8 OLI instrument designed, and only the band combination can be charged on the detection methodology. The coastal band penetrates in the water and supports aquatic vegetation identification. The use of the coastal band for the classification instead of the usual red band increases the spectral differences of the classes and helps to reach maximum limit of the detection. The manual classification procedure using predefined objects (due to OBIA analysis) is an important aspect since the analyser is focused on a group of pixels with

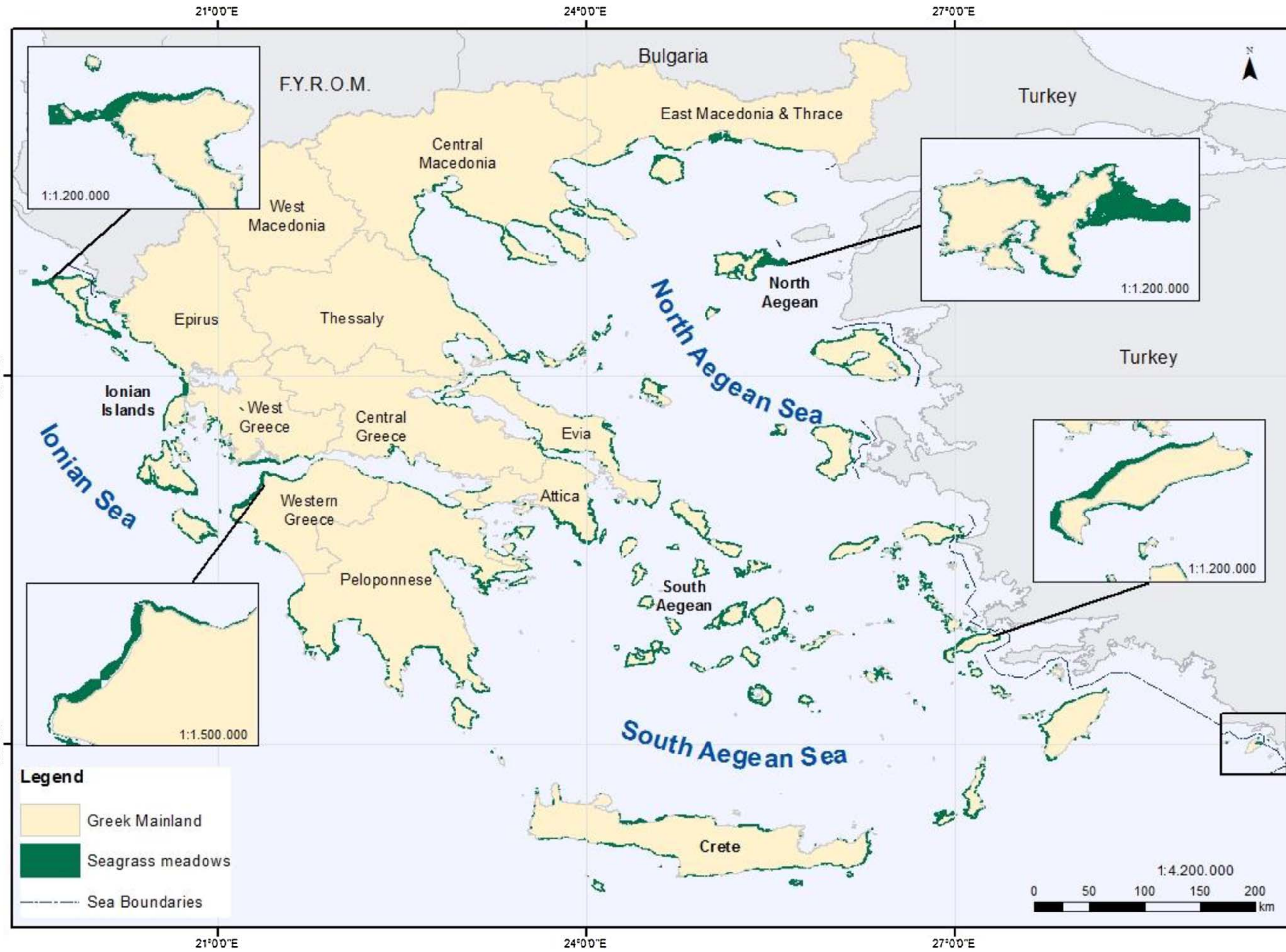

Fig. 6. Seagrass meadows detected in Greek territorial waters.

similar characteristics and not on single pixels. Last but not least, the knowledge of the area and the classification experience of the analyser are of high importance and determine to a large extent the positioning of the deepest limit. A dedicated study is required for defining the deepest limit of the seagrass meadows which can be seen in satellite images, using specific points with high positional accuracy *i.e.* DGPS and multibeam measurements.

3.2. Accuracy analysis

Table 2 presents the common seagrass area between the detected vector and the earlier mapping of the Natura 2000 sites (in km^2 and in %), as well as the total accuracy of the classification for the Greek coastal Natura 2000 sites. The mean total accuracy for all 62 sites was 76.3%. Three sites (5% of the reference data) were mapped with a total accuracy of less than 50%, 15 (24% of the reference data) with an accuracy of 50–69%, 20 (32% of the reference data) with an accuracy of 70–80%, and 24 (38% of the reference data) with an accuracy greater than 80%. Overall accuracies less than 50% indicate worse-than-random performance of the classifier.

Although the total accuracy was considered satisfactory in terms of the number of satellite images used, the common seagrass areas between the detected vector and the earlier mapping of the Natura 2000 sites were not consistent with the total accuracy. In some cases, the total accuracy followed the overall trend of the common seagrass percentage (e.g. GR1130009, GR2420004, GR4110001, GR4210001) and even in seven cases the common seagrass percentage was higher than the total accuracy (e.g. GR1150007, GR3000005, GR4210001). However, in most cases the difference between the detected vectors and the earlier Natura 2000 vector was significant. This finding can be understood if we examine the area of each site and the quality of the reference dataset. Natura sites with small seagrass coverage had the lager differences (e.g. GR4210011, GR4210009, GR4340008), which can be explained if we take into account i) the fragmented seagrass coverage in these small areas, ii) the difference of the comparison data type (vector for Natura 2000 and raster from satellite images) and iii) the possible mislocation between the reference and the satellite images.

3.3. Case studies

Although 70% of the reference sites present acceptable total accuracy values (70–100%), the low accuracy of the remaining sites, and the behavior of the common seagrass area between the detected vector and the Natura 2000 sites, were examined. Three Natura 2000 sites have been selected as representatives for a better clarification of the accuracies and their impacts on the produced vectors. The first site (GR4110001) contains the largest seagrass meadow of the study area and represents cases with medium to high total accuracy values. The second (GR4340005) is a small site with a high total accuracy, and the third is an average-size site (GR1270009) with a low total accuracy.

3.3.1. Case study of GR411001 site

The GR4110001 site is on the northeastern part of Greece on Lemnos Island, directly opposite the Dardanelles Strait. The total site covers an area of 182 km^2, of which 52 km^2 extend inland, and 130 km^2 are in the sea. The seagrass coverage in the reference dataset is 115 km^2, consisting of *P. oceanica* meadows. It is the largest single area mapped in Greece and is almost one-fifth of the total area of the

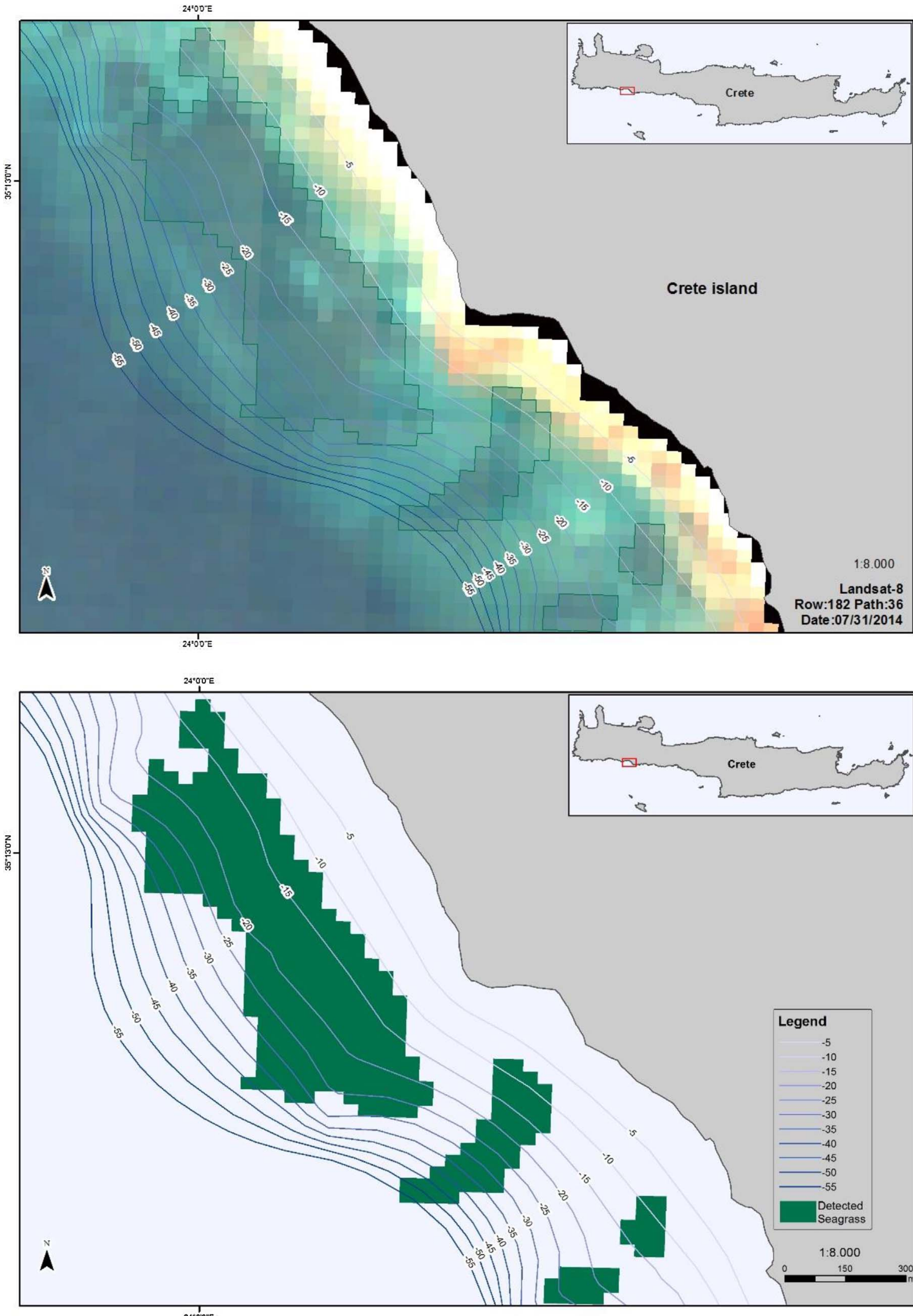

Fig. 7. Example with one of the deepest seagrass meadows detected (top: satellite image after pre-processing, down: detected seagrass area).

reference seagrass in the country.

The large seagrass meadow can be seen in the Landsat-8 image after the preprocessing procedure (Fig. 8). However, due to the high turbidity in the area and the relevant deep waters, a careful image selection has been necessary for revealing the limits of the meadow. Fig. 8 shows the classification results and the reference vector line as the

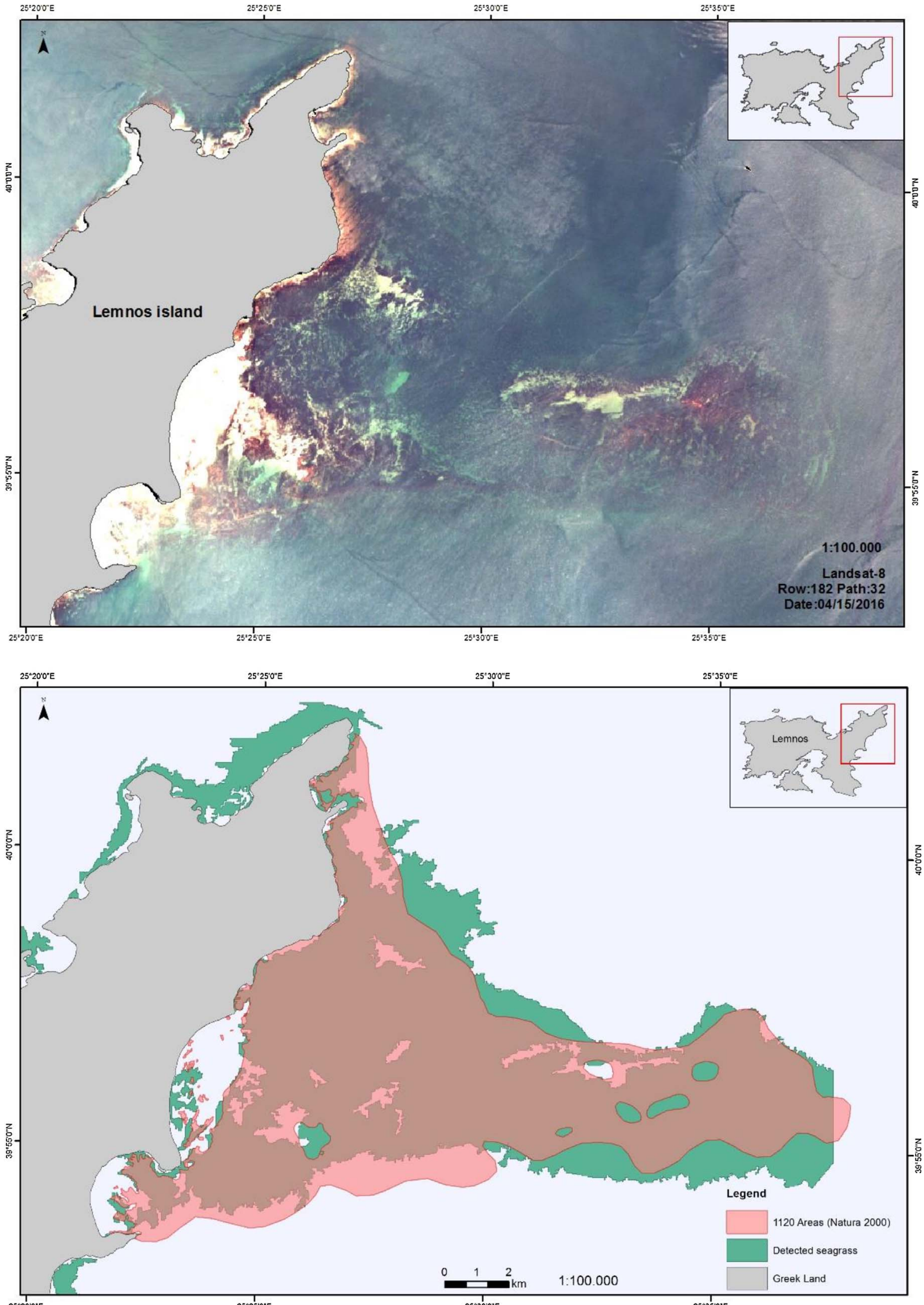

Fig. 8. Example of the GR4110001 case study (top: satellite image after pre-processing, down: detected seagrass area and Natura 2000 reference).

Table 3
Accuracy matrix of the Natura 2000 GR4110001 site.

Natura site code			GR4110001
	Reference Seagrass (km^2)	Reference Not Seagrass (km^2)	User accuracy
Predicted Seagrass (km^2)	95.39	5.15	0.95
Predicted Not Seagrass (km^2)	19.68	9.88	0.67
Producer accuracy	0.83	0.52	
Total accuracy: 0.81		F1 score: 0.88	

green area and the red polygon, respectively. The two areas are relatively close, and a satellite image can approximate the real borders of the meadow.

Table 3 presents the accuracy matrix between the reference Natura 2000 vector and the produced vector. The total accuracy of the comparison (80.92%) reveals relatively high accuracy for the two classes (seagrass and non-seagrass areas). By comparing only the common seagrass areas of the two vectors, 95.39 km^2 of the 115 km^2 of the reference are found to be common (82.73%). The good correlation between the detected seagrass area and the reference seagrass area can also be seen by the F1 score (0.88), which considers both precision (seagrass positive predictive value) and recall (seagrass true positive rate) for computing the 0–1 score. This is an example of a large area with extensive seagrass meadows and a relatively high total accuracy. The percentages of the total accuracy and the common seagrass are very close, because the mapped reference area is mostly covered with seagrass. In contrast, the next two examples represent medium and small sizes of reference meadows, with low and high accuracies, respectively.

3.3.2. Case study of GR434005 site

The second example is the GR4340005 site on the southwestern part of Crete Island, named Ormos Sougias. It covers an area of 30.4 km^2, of which 19.6 km^2 are on land and 10.8 km^2 are in the sea. The marine component extends to the Libyan Sea and includes *Posidonia* beds (category 1120), a small area with vegetated soft bottoms (category 119B), reefs (category 1170), rocks, and steep cliffs. The seagrass coverage in the reference dataset is small, only 0.07 km^2 (Table 4), of which *P. oceanica* meadows cover 0.05 km^2, and the rest comprises vegetated soft bottoms (0.02 km^2).

Fig. 9 illustrates the results of the detection. The seagrass meadows are visible in the Landsat-8 image after the preprocessing procedure—even in such deep waters. The comparison of the seagrass classification results and the reference vector line shows the produced vector as covering a significantly larger area than the reference one. These seagrass areas are visible in the satellite image but not mapped in the reference dataset. The small area of the 119 B category on the eastern part of the site is also mislocated between the two vectors. However, part of the reference *Posidonia* beds match the produced vector, and in combination with the very large area of the not-seagrass category a total accuracy of 97.50% was calculated. On the contrary, the direct comparison of the common seagrass areas reveals 43.40% accuracy, since only 0.03 km^2 of 0.07 km^2 are the same between the two vectors. The large difference in the area coverage of the two categories results also in the low F1 score (0.18) due to the low precision value of the seagrass category.

Table 4
Accuracy matrix of the Natura 2000 GR4340005 site.

Natura site code			GR4340005
	Reference Seagrass (km^2)	Reference Not Seagrass (km^2)	User accuracy
Predicted Seagrass (km^2)	0.03	0.22	0.12
Predicted Not Seagrass (km^2)	0.05	10.50	0.00
Producer accuracy	0.38	0.02	
Total accuracy: 0.98		F1 score: 0.18	

This is an example of a relatively small site with limited seagrass meadow. The mapping in terms of total accuracy is considered almost perfect, mainly because the reference dataset of the non-seagrass category is completely mapped from the satellite images. However, less than half of the seagrass area was correctly identified. The seagrass accuracy of this site is limited by the seagrass meadows observed in satellite images but not included in the reference data. The GR4340005 site is a very good example of using satellite images for marine habitat mapping in isolated areas.

3.3.3. Case study of GR1270009 site

The GR1270009 site is in the northern Aegean Sea and includes seagrass meadows with high density. Most of the site is in the marine area and is covered by the Natura 2000 categories: *Posidonia* beds (1120), sandbanks that are slightly covered by sea water all the time (1110), unvegetated soft bottoms (119A), and vegetated soft bottoms (119B). The seagrass coverage in the reference dataset is 9.13 km^2, consisting of *P. oceanica* meadows (3.11 km^2) and the rest of vegetated soft bottoms (6.02 km^2).

Fig. 10 illustrates the results of the detection. The seagrass meadows are visible in the Landsat-8 image after the preprocessing procedure. The classification results and the reference vector line are also added as separate layers for visual comparison of the method's accuracy. This is the site with a lower overall accuracy. The satellite image does not match the *P. oceanica* meadows (1120), and only some of the vegetated soft bottoms are correctly classified.

The comparison of the reference vector and the produced vector reveals a relatively low total accuracy, almost 30% (Table 5) and low F1 score (0.24). By comparing the common seagrass areas of the two vectors, only 1.24 km^2 of 9.13 km^2 of the reference were found to be common (13.63%). This is an example of the method's limitation, and it is caused by the wrong selection of the satellite image. The reference seagrass areas are more visible in the satellite images taken on other dates with cleaner waters.

4. Discussion

4.1. Implications for conservation and marine spatial planning

Systematic conservation planning requires sound and verified knowledge of the distribution of ecological features (Lourie and Vincent, 2004). As the distribution of species is usually difficult and expensive to obtain, habitats are often used as surrogates of biodiversity distribution for the identification of priority areas for conservation in coastal ecosystems (Giakoumi et al., 2013; Ward et al., 1999). Hence, satellite imaging for mapping marine habitats is a valuable tool providing a cost-effective way to create distribution maps of shallow habitats at large spatial scales. The range map of *P. oceanica* in the Mediterranean Sea from the International Union for Conservation of Nature (IUCN) depicts a uniform presence within a very wide and unrealistic coastal buffer zone (Pergent et al., 2012), including areas from which *P. oceanica* is known to be absent (Giakoumi et al., 2013). Relying on such coarse datasets could misinform conservation planning (Levin et al., 2014). There is a need to increase efforts on a regional scale for finer maps of marine habitats; satellite imaging can substantially contribute towards that direction.

With the present study, the information on the seagrass coverage in Greece is dramatically improved. The seagrass vector provided here describe and quantify for the first time the extent and the spatial

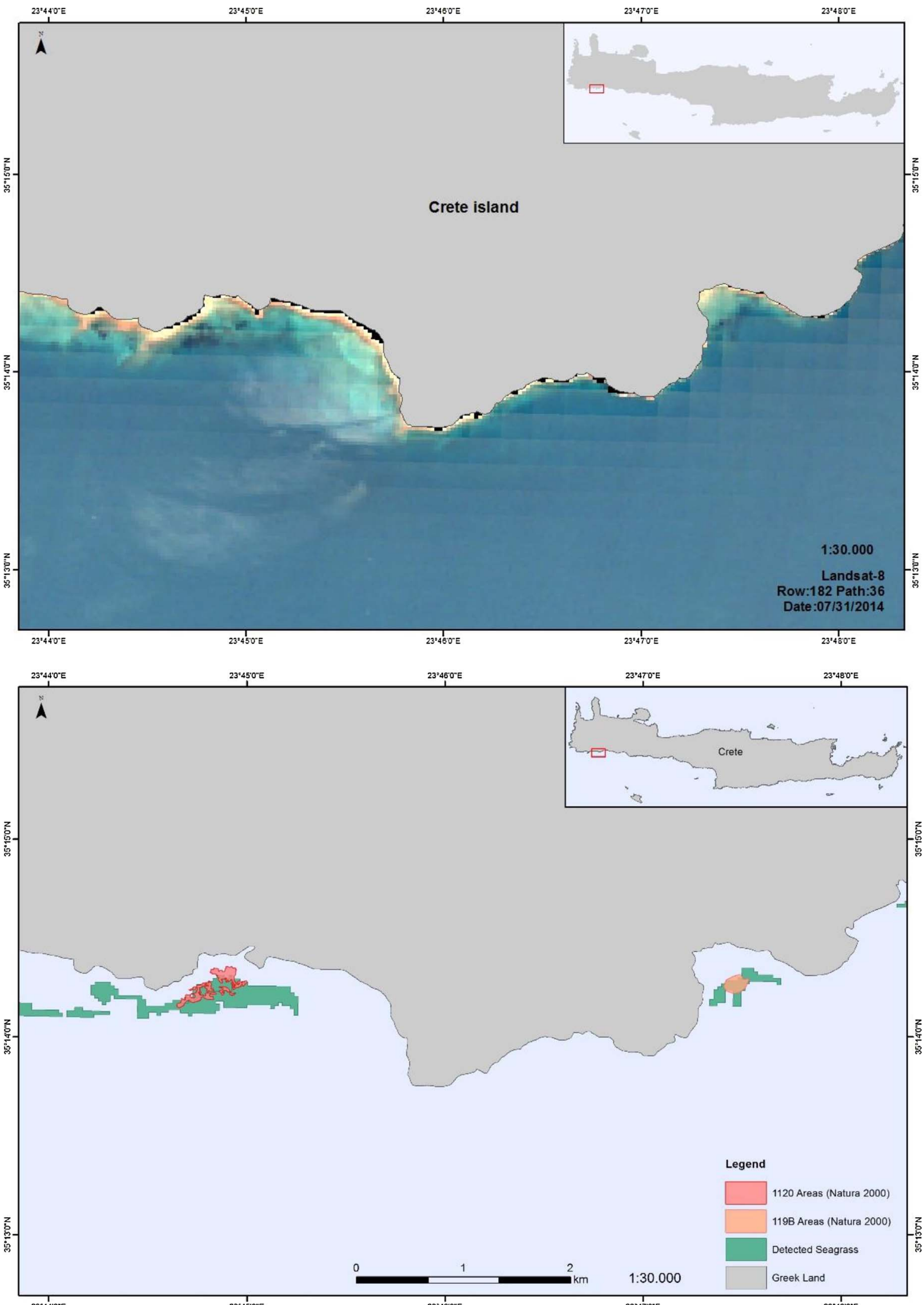

Fig. 9. Example of the GR4340005 case study (top: satellite image after pre-processing, down: detected seagrass area and Natura 2000 reference).

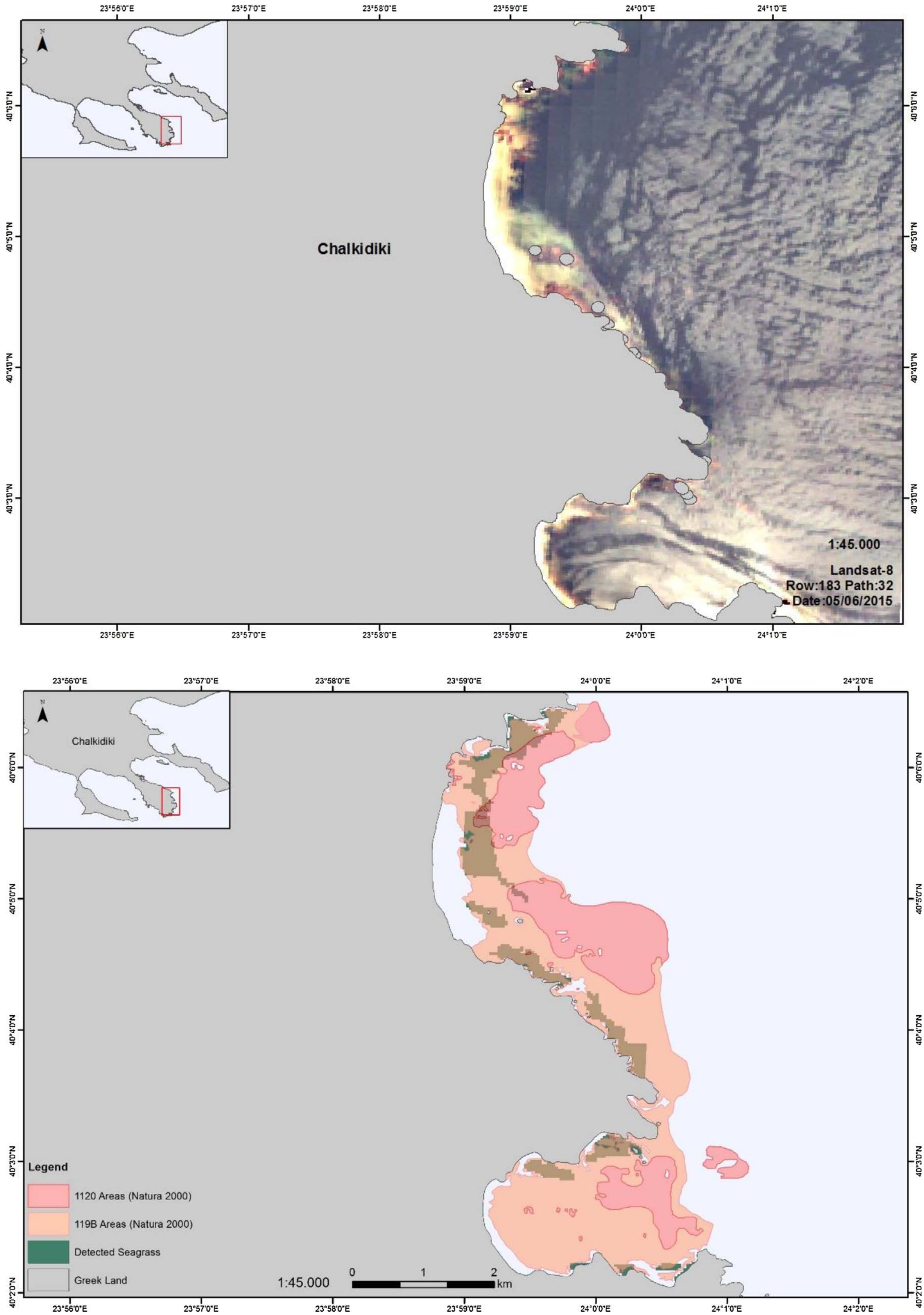

Fig. 10. Example of the GR1270009 case study (top: satellite image after pre-processing, down: detected seagrass area and Natura 2000 reference).

Table 5
Accuracy matrix of the Natura 2000 GR1270009 site.

Natura site code			GR1270009
	Reference Seagrass (km^2)	Reference Not Seagrass (km^2)	User accuracy
Predicted Seagrass (km^2)	1.24	7.90	0.14
Predicted Not Seagrass (km^2)	0.09	2.11	0.04
Producer accuracy	0.93	3.75	
Total accuracy: 0.30		F1 score: 0.24	

distribution of seagrass meadows in Greek waters. Many previously unknown seagrass meadows in the country were located, mapped and quantified. The largest seagrass meadows were highlighted and priority conservation sites for the protection of seagrasses and their related ecosystem services (Liquete et al., 2013) can now be identified. Also, the present study has a large impact on Mediterranean level, since it fills a large gap on our knowledge of seagrass coverage in the eastern Mediterranean, as the herein presented dataset represents more than half of the missing data in the Mediterranean Sea.

P. oceanica beds are considered a priority habitat for conservation by the EU Habitats Directive and the Barcelona Convention. They function as important nursery grounds for many species (Francour, 1997), are one of the most productive marine ecosystems, and provide a multitude of ecosystem services such as food provision, coastal protection, carbon sequestration, water purification and life cycle maintenance (Liquete et al., 2013). However, they are threatened by cumulative impacts (Giakoumi et al., 2015) and are declining rapidly (Waycott et al., 2009). Despite the recommendation of the European Topic Centre on Biological Diversity for the protection of > 60% of the *P. oceanica* meadows (ETC/BD, 2010), the established protected areas in the study area are far from reaching this spatial target. This was mainly due to the absence so far of a complete distribution map of *P. oceanica*. The maps herein produced will make it possible to assess the level of protection of *P. oceanica* beds in Greek seas and appropriately expand conservation efforts to reach specific operational targets.

The vectors produced for each administrative region in Greece are extremely valuable for conservation and management. European and Greek environmental legislation recognizes seagrass meadows as priority habitats, where destructive activities such as trawling are banned. In the absence of mapping, surveillance and enforcement of such restrictions was impossible but now Greek prefectures have a good overview of the area they need to monitor and protect. Furthermore, knowledge of the distribution of seagrass meadows is vital information for systematic conservation planning especially in view of the obligation of Greece to establish maritime spatial plans by 2021 according to the EU Regulation 2014/89/EU. A prerequisite for planning is the good knowledge of the distribution of habitats and thus the present results fill an important gap. Part of the herein presented seagrass maps has already been used in the framework of the MARISCA project (http://www.marisca.eu) 'MARItime Spatial planning for the protection and Conservation of the biodiversity in the Aegean sea', which very recently proposed a network of marine protected areas and a zoning system in the Aegean sea for the conservation of all important and vulnerable habitats and species (Katsanevakis et al., 2017).

Due to the very high cost of other mapping approaches that are based on extensive field work with vessels, echosounders, cameras and divers, the seagrass beds of Greece (as well as of many other Mediterranean countries) had remained unmapped. Hence, the approach herein presented is promising for large scale mapping and monitoring of seagrass beds in many other regions to cover the existing information gaps. Furthermore, it is valuable to monitor trends in the spatial extent of seagrass beds by comparing images of different years and thus to assess the rates of change and the effectiveness (or ineffectiveness) of conservation actions.

4.2. Remote sensing considerations

The seagrass map and the product accuracy may have been affected by a number of potential sources of errors in the image analysis and/or the reference data. One of the major concerns is the large time gap between the reference maps (created in 1998–2001) and the acquired satellite images (2014–2015 acquisition period). Moreover, although most of the coverage area of the reference Natura 2000 maps contains *P. oceanica,* which can remained unchanged for many decades if it is not affected by human pressure, several other species with mutable behaviors have been included in the 119 B category (e.g., *C. nodosa*). Therefore, changes had possibly occurred in the interval between image acquisition and ground truthing. However, taking into account the extent of the seagrass distribution in the present study and given the large time differences previously reported (around 8 years in Torres-Pulliza et al., 2013; 16 years in Gullström et al., 2006; 25 years in Knudby et al., 2010), we believe that the bias in our assessment due to temporal changes is low.

Second, the reported total accuracy is based on the comparison of the two classes: seagrass and non-seagrass. While the extent of the seagrass class is straightforward, that of the non-seagrass class depends on the size of the reference Natura 2000 sites, since their external borders are used as the area definition. The percentage of the common seagrass area of the produced vector and the reference data set is a better metric for the accuracy (however, the overall area of the reference seagrass meadow is also very important for the accuracy assessment). From the above-mentioned case studies and the relevant accuracy tables, we observe that the seagrass match depends on the size of the seagrass meadow. A direct comparison of only the seagrass class is misleading in terms of the percentage accuracy for small and medium-sized seagrass meadows due to uncertainties in the mapping accuracy of the reference data.

Third, uncertainties were introduced due to manual classification as a result of strong limitations on the spectral signatures of seagrass meadows. Satellite images were initially preprocessed to achieve similar reflectance values as much as possible. However, due to different environmental conditions during the image acquisition (*i.e.*, water turbidity, wind-speed direction, and wave-height surf), the reflectance values presented large differences. Manual classification was necessary for achieving high seagrass accuracy detection due to this difference.

5. Conclusions and perspectives

This study has confirmed the ability to produce reliable coverage data on the spatial distribution of seagrass meadows for large-scale ecological and conservation studies using satellite images. The produced maps are ideal for identifying priority conservation sites to help experts develop conservation strategies and design a resilient network of protected marine areas in Greece. We used a total of 50 Landsat-8 (OLI) images, covering the extent of the Greek seas with high differences in geomorphology, structure, and seagrass bed extent. For the first time, Greek waters were mapped for the presence/absence of seagrass meadows in the whole spatial domain. The resulting data were used as inputs for producing the percentage of seagrass coverage cells of 1 km to apply to national legislation. The produced vectors are provided freely for public use, toward sustainable marine spatial planning, local development projects, and conservation studies, and are available on the University of Aegean's Marine Remote Sensing Group web page (http://mrsg.aegean.gr/).

The results are encouraging in terms of accuracies and mapping large seagrass meadows. The mean accuracy of 76.3% was produced when comparing our results against the previously mapped 62 sites. The detection accuracy is consistent with those of previously published studies. However, the available reference data are outdated and present uncertainties. Therefore, there is an urgent need for updated, accurate reference data (*in situ*, side scan sonars, ROVs, and drones) on a country scale, freely available for scientific studies.

Accurate seagrass mapping using remote sensing data in coastal areas (*i.e.*, in relatively shallow areas) was previously proven. However, the present study shows for the first time that satellite images can be used for seagrass mapping–even in deeper waters. Extensive areas of seagrass beds along the Greek shoreline, some of them reaching depths of ~ 40 m, have been successfully detected. In such areas, there is a vital need to discover methods for selecting the proper satellite image with the highest water clarity and visibility. The use of time-series analysis of the satellite images is a key factor for proper image selection. The sea status is a dynamic phenomenon, and a strong pre-processing phase is required to select proper images for classification. Moreover, in such waters, the seagrass signature is differentiated in terms of depth. A better separation of classes would be possible, taking into account the depth contours.

The next steps include the use of 10-m optical bands of Sentinel-2 data to improve the spatial resolution of the produced vectors and the time-series analysis to select the proper image (*i.e.*, the image with the lowest water turbidity) in each subarea of the study. Last but not least, in using the detected seagrass vectors, a new study is required to re-examine the spectral signatures of the seagrasses in different depths and in different regions. In parallel, further map validation with dedicated *in situ* measurements (*i.e.*, high-resolution Unmanned Aerial Vehicle-UAV orthophoto maps and multibeam side scan sonar) will help highlight the weaknesses and the strengths of our product.

Acknowledgments

The seagrass mapping was supported by a contract with the Hellenic Center for Marine Research (HCMR) and the Fisheries Research Institute (HAO-DEMETER) within the framework of the Seagrass Meadows Mapping in the Greek Seas project, co-funded by the Greek government and the EU (Fisheries Operational Program), and by the MARISCA project (www.marisca.eu), co-funded (85%) by the EEA Grants, 2009–2014, and the Public Investments Program of the Hellenic Republic (15%).

References

Boudouresque, C.F., Bernard, G., Pergent, G., Shili, A., Verlaque, M., 2009. Regression of Mediterranean seagrasses caused by natural processes and anthropogenic disturbances and stress: a critical review. Bot. Mar. 52. http://dx.doi.org/10.1515/BOT.2009.057.

Congalton, R., Green, K., 2008. Assessing the Accuracy of Remotely Sensed Data: Principles and Practices, second edi. ed. CRC Press.

ETC/BD, 2010. European Topic Centre on Biological Diversity.

Francour, P., 1997. Fish assemblages of *Posidonia oceanica* beds at port-cros (France, NW Mediterranean): Assessment of composition and long-term fluctuations by visual census. Mar. Ecol. 18, 157–173. http://dx.doi.org/10.1111/j.1439-0485.1997.tb00434.x.

Gerakaris, V., Panayotidis, P., Tsiamis, K., Nikolaidou, A., Economou-Amili, A., 2014. Posidonia oceanica meadows in Greek seas: lower depth limits and meadow densities. In: 5th Mediterranean Symposium on Marine Vegetation. Portorož, Slovenia, 27–28 October 2014. pp. 70–73.

Gerakaris, V., 2017. Grasslands of the Marine Angiosperm *Posidonia Oceanica* (L.) Delile as Item Description of the Greek Seas. PhD Thesis. (Athens).

Giakoumi, S., Sini, M., Gerovasileiou, V., Mazor, T., Beher, J., Possingham, H.P., Abdulla, A., Çinar, M.E., Dendrinos, P., Gucu, A.C., Karamanlidis, A.A., Rodic, P., Panayotidis, P., Taskin, E., Jaklin, A., Voultsiadou, E., Webster, C., Zenetos, A., Katsanevakis, S., 2013. Ecoregion-based conservation planning in the mediterranean: dealing with large-scale heterogeneity. PLoS One 8. http://dx.doi.org/10.1371/journal.pone.0076449.

Giakoumi, S., Halpern, B.S., Michel, L.N., Gobert, S., Sini, M., Boudouresque, C.-F., Gambi, M.-C., Katsanevakis, S., Lejeune, P., Montefalcone, M., Pergent, G., Pergent-Martini, C., Sanchez-Jerez, P., Velimirov, B., Vizzini, S., Abadie, A., Coll, M., Guidetti, P., Micheli, F., Possingham, H.P., 2015. Towards a framework for assessment and management of cumulative human impacts on marine food webs. Conserv. Biol. 29, 1228–1234. http://dx.doi.org/10.1111/cobi.12468.

Green, E.P., Short, F., 2003. World Atlas of Seagrasses, Prepared by the UIMEP World Conservation Monitoring Centre. University of California Press, Berkeley USA. http://dx.doi.org/10.1515/BOT.2004.029.

Green, E.P., Mumby, P.J., Clark, C.D., Edwards, T.M., 2000. Remote Sensing Handbook for Tropical Coastal Management, Coastal Management Sourcebooks. UNESCO Publishing, Paris.

Gullström, M., Lundén, B., Bodin, M., Kangwe, J., Öhman, M.C., Mtolera, M.S.P., Björk, M., 2006. Assessment of changes in the seagrass-dominated submerged vegetation of tropical Chwaka Bay (Zanzibar) using satellite remote sensing. Estuar. Coast. Shelf Sci. 67, 399–408. http://dx.doi.org/10.1016/j.ecss.2005.11.020.

Hedley, J., Russell, B., Randolph, K., Dierssen, H., 2016. A physics-based method for the remote sensing of seagrasses. Remote Sens. Environ. 174, 134–147. http://dx.doi.org/10.3390/rs8020118.

Hossain, M.S., Bujang, J.S., Zakaria, M.H., Hashim, M., 2015. The application of remote sensing to seagrass ecosystems: an overview and future research prospects. Int. J. Remote Sens. 36, 61–114. http://dx.doi.org/10.1080/01431161.2014.990649.

Katsanevakis, S., Sini, M., Koukourouvli, N., Markantonatou, V., Topouzelis, K., Giakoumi, S., Koutsoubas, D., Hasiotis, T., Manoutsoglou, E., Velegrakis, A., Papakonstantinou, A., Maniopoulou, M., Andreadis, O., Dailianis, T., Gerovasileiou, V., Ragkousis, M., Tsokaros, P., Bakogianni, M., Christofidis, S., Vasilopoulou, V., Karachle, P., Gadolou, E., Stithou, M., Kavadas, S., Maina, I., Panayotides, P., Papadopoulos, E., Charalambous, I., Buhl-Mortensen, L., Gonzalez-Mirelis, G., 2017. Marine Spatial Planning in the Aegean Sea for the Protection and Conservation of Biodiversity (Marisca). Final Project Report.

Knudby, A., Newman, C., Shaghude, Y., Muhando, C., 2010. Simple and effective monitoring of historic changes in nearshore environments using the free archive of Landsat imagery. Int. J. Appl. Earth Obs. Geoinf. 12, 116–122. http://dx.doi.org/10.1016/j.jag.2009.09.002.

Levin, N., Coll, M., Fraschetti, S., Gal, G., Giakoumi, S., Göke, C., Heymans, J., Katsanevakis, S., Mazor, T., Öztürk, B., Rilov, G., Gajewski, J., Steenbeek, J., Kark, S., 2014. Biodiversity data requirements for systematic conservation planning in the Mediterranean Sea. Mar. Ecol. Prog. Ser. 508, 261–281. http://dx.doi.org/10.3354/meps10857.

Liquete, C., Piroddi, C., Drakou, E.G., Gurney, L., Katsanevakis, S., Charef, A., Egoh, B., 2013. Current status and future prospects for the assessment of marine and coastal ecosystem services: a systematic review. PLoS One 8, e67737. http://dx.doi.org/10.1371/journal.pone.0067737.

Lourie, S.A., Vincent, A.C.J., 2004. Using biogeography to help set priorities in marine conservation. Conserv. Biol. http://dx.doi.org/10.1111/j.1523-1739.2004.00137.x.

Lyons, M.B., Phinn, S.R., Roelfsema, C.M., 2012. Long term land cover and seagrass mapping using Landsat and object-based image analysis from 1972 to 2010 in the coastal environment of South East Queensland, Australia. ISPRS J. Photogramm. Remote Sens. 71, 34–46. http://dx.doi.org/10.1016/j.isprsjprs.2012.05.002.

Matthew, M.W., Adler-Golden, S.M., Berk, A., Felde, G., Anderson, G.P., Gorodetzky, D., Paswaters, S., Shippert, M., 2002. Atmospheric correction of spectral imagery: evaluation of the FLAASH algorithm with AVIRIS data. Applied Imagery Pattern Recognition Workshop, 2002. Proceedings. IEEE Comput. Soc 157–163. http://dx.doi.org/10.1109/AIPR.2002.1182270.

Monaco, M.E., Anderson, S.M., Battista, T.A., Kendall, M.S., Rohmann, S.O., Wedding, L.M., Clarke, A.M., 2012. National Summary of NOAA's Shallow-water Benthic Habitat Mapping of U. S. Coral Reef Ecosystems. NOAA Technical Memorandum NOS NCCOS 122. Prepared by the NCCOS Center for Coastal Monitoring and Assessment Biogeography Branch. Silver Spring.

Mumby, P., Hedley, J., Chisholm, J., Clark, C., Ripley, H., Jaubert, J., 2004. The cover of living and dead corals from airborne remote sensing. Coral Reefs 23, 171–183. http://dx.doi.org/10.1007/s00338-004-0382-1.

Panayiotidis, P., Drakopoulou, P., Siakavara, A., Banks, A., Orphanides, S., Tsianga, E., Haritonidis, S., Tsirika, A., 2002. Mapping of marine habitat types in 67 regions of the network Natura 2000. Proceedings of the 2nd Panhellenic Congress Management and Improvement of Coastal Zones 437–444.

Pergent, G., Bazairi, H., Bianchi, C.N., Boudouresque, C.F., Buia, M.C., Clabaut, P., Harmelin-Vivien, M., Mateo, M.A., Montefalcone, M., Morri, C., Orfanidis, S., Pergent-Martini, C., Semroud, R., Serrano, O., Verlaque, M., 2012. Mediterranean Seagrass Meadows: Resilience and Contribution to Climate Change Mitigation, A Short Summary. (Gland, Switzerland and Málaga, Spain).

Poursanidis, D., Barnias, A., Petros, L., 2014. Assessment of the conservation status of *Posidonia oceanica* meadows in the Samaria national park, an MPA in crete, Greece. In: Proceedings of the 5th Mediterranean Symposium on Marine Vegetation. Portorož, Slovenia, 27–28 October 2014. pp. 143–148.

Sakellariou, D., Alexandri, M., 2007. Geomorphology of the Hellenic sea-floor. In: Papaconstantinou, C., Zenetos, V., Vassilopoulou, V., Tserpes, G. (Eds.), State of Hellenic Fisheries. HCMR.

Sakellariou, D., Lykousis, V., Karageorgis, A., Anagnostou, C., 2005. In: Papathanasiou, E., Zenetos, A. (Eds.), Geomorpholgy and Tectonic Structure. H. publications (Ed.), State of the Hellenic Marine Environment, SoHelME, pp. 360.

Telesca, L., Belluscio, A., Criscoli, A., Ardizzone, G., Apostolaki, E.T., Fraschetti, S., Gristina, M., Knittweis, L., Martin, C.S., Pergent, G., Alagna, A., Badalamenti, F., Garofalo, G., Gerakaris, V., Louise Pace, M., Pergent-Martini, C., Salomidi, M., 2015. Seagrass meadows (*Posidonia oceanica*) distrution and trajectories of change. Sci. Rep. 5, 12505. http://dx.doi.org/10.1038/srep12505.

Torres-Pulliza, D., Wilson, J.R., Darmawan, A., Campbell, S.J., Andréfouët, S., 2013. Ecoregional scale seagrass mapping: a tool to support resilient MPA network design in the Coral Triangle. Ocean Coast. Manage. 80, 55–64. http://dx.doi.org/10.1016/j.ocecoaman.2013.04.005.

USGS, 2016. Landsat 8 (L8) Data Users Handbook.

Wabnitz, C.C., Andréfouët, S., Torres-Pulliza, D., Müller-Karger, F.E., Kramer, P. a., 2008. Regional-scale seagrass habitat mapping in the Wider Caribbean region using Landsat sensors: applications to conservation and ecology. Remote Sens. Environ. 112,

3455–3467. http://dx.doi.org/10.1016/j.rse.2008.01.020.
Ward, T.J., Vanderklift, M.A., Nicholls, A.O., Kenchington, R.A., 1999. Selecting marine reserves using habitats and species assemblages as surrogates for biological diversity. Ecol. Appl. 9, 691–698. http://dx.doi.org/10.1890/1051-0761(1999)009[0691:SMRUHA]2.0.CO;2.
Waycott, M., Duarte, C.M., Carruthers, T.J.B., Orth, R.J., Dennison, W.C., Olyarnik, S., Calladine, A., Fourqurean, J.W., Heck, K.L., Hughes, A.R., Kendrick, G.A., Kenworthy, W.J., Short, F.T., Williams, S.L., 2009. Accelerating loss of seagrasses across the globe threatens coastal ecosystems. Proc. Natl. Acad. Sci. 106, 12377–12381. http://dx.doi.org/10.1073/pnas.0905620106.
Wolf, A., 2010. Using WorldView 2 Vis-NIR MSI Imagery to Support Land Mapping and Feature Extraction Using Normalized Difference Index Ratios Worldview 83900N–83900N–8. http://dx.doi.org/10.1117/12.917717.